Sequentially Switched Antenna Array and Application to a WiMAX System

Julian Webber, Satoshi Tsukamoto, Takahiro Maeda, and Tomoaki Kumagai
Advanced Telecommunications Research International, 2-2-2, Hikaridai, Seika-cho, Kyoto, 619-0288, Japan
{**jwebber, tsukamoto, maeda, t.kumagai**}**@atr.jp**
Shinichiro Yamamoto, and Satoru Aikawa
Graduate School of Engineering, University of Hyogo, 2167 Syosya, Himeji-shi, Hyogo, 671-2280 Japan
{**yamamoto, aikawa**}**@eng.u-hyogo.ac.jp**

***Abstract*—A continuous-switching type array antenna receiver has been proposed in order to reduce the deterioration due to fast-fading channel variations and improve communication performance. The receive antennas are placed in a linear array, and by sequentially switching the elements in the opposite direction to the direction of the train travel, it has been possible to fix the signal receiving point virtually. Through the development of a scale-model experiment of high-speed movement using the prototype antenna, in this paper we show that it is possible through optimized antenna element selection and appropriate signal processing to reduce the fading rate and improve the performance of an OFDM system. A software simulation based on the Worldwide Interoperability for Microwave Access (WiMAX) physical layer parameters was made and data transmitted at RF in a 5 MHz bandwidth with symbol rate appropriately scaled to simulate a range of fading speeds. The receive antenna array consisting of eight elements traverses a track at a virtual speed of 180 km/h and the error rate performances with and without switching are compared.**

***Index Terms*—**Linear array antenna, fast-fading, antenna switching, OFDM, WiMAX, experiment.

I. Introduction

During the last decade, use of mobile devices including smart phones and tablets has increasingly become widespread. These devices are pervasive in coaches, trains, and airplanes and often for bandwidth hungry applications such as video streaming. The phenomenal increase in mobile data usage is set to continue with a forecast of a ten-fold increase over the next 5 years [1]. In order to cope with this large increase, capacity enhancement of the entrance line is required.

High-order multi-level modulation such as 1024 QAM and use of higher frequency band communications are candidates to enable a sustained increased data-rate to moving vehicles. However, the fundamental and limiting problem of deep fading over very short distances still needs to be overcome to realize the full benefit of these schemes. Performance degradation caused by fast fading is more significant than the use of low-order modulation and current frequency band usage. By reducing the fading rate whilst traveling at high speeds, data-rates can be significantly increased.

Various systems have been proposed in the recent literature to improve the communications performance on high-speed trains. Optimization of antenna directional gain by 5-10 dB and reduction in Doppler spread was demonstrated in [2]. An integrated satellite and terrestrial system similar to the IEEE802.16a physical layer was proposed in [3] for speeds up to 100 km/h. Sharing signals from remote radio heads in order to improve handover between base-stations has been proposed in [4]. Channel estimation techniques for WiMAX systems were explored in [5], where it was shown that at the high speed of 345 km/h Doppler significantly affects the performance and, advanced adaptive coding and modulation techniques were proposed solutions. Doppler spread characteristics and practical LTE performance results along viaducts were studied for the Chinese Harbin-Dalian railway for speeds up to 370 km/h in [6]. Throughput performance results and propagation loss returns for a WiMAX system on the Taiwanese Shinkansen are reported in [7].

When a large number of terminals are used in a vehicle, it is best for terminal users if a relay system with local access points is deployed [8]. If all the terminals connect to a ground base station via the relay system, congestion can be avoided by reducing the handover frequency and results in an efficient usage of the radio resource. This kind of system is already deployed in super-express trains including the Japanese bullet train for example.

In this paper, we demonstrate the application of the sequentially switched linear array antenna which has the ability to virtually cancel out the movement of the antenna system. An eight-elements linear array antenna with various element spacing's was designed in order to research the characteristics and performance benefits with a scale model of the entrance line as shown in Fig. 1.

The layout of this paper is as follows. The system concept is described in Section II. The proposed switched antenna and switching characteristics are presented in Section III. A WiMAX system simulation using experimental data from the array is presented in Section IV. Further work is outlined in Section V and a conclusion drawn in Section VI.

II. System Concept

The conceptual diagram of the proposed receiver using the linear array antenna is shown in Fig. 2. The antenna array is positioned on the train roof and the array elements are aligned along the direction of the train travel. Initially, the first element is selected and is shown as time 1a in the figure. After a

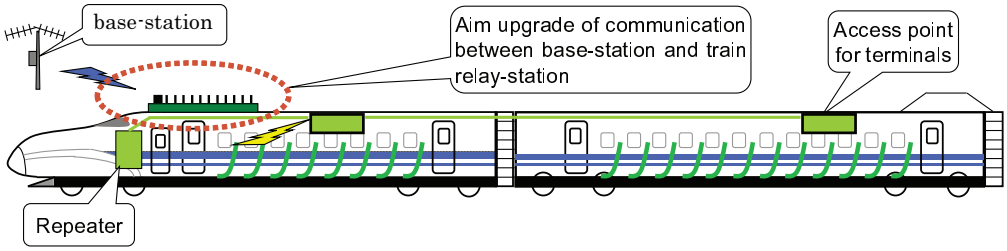

Fig. 1. An example image of a target system.

short period of time, the second element becomes aligned to the same position as the first element was, and the second element is selected. With suitable switch timing relative to the trains speed, the same receiving point relative to the ground is kept, and the selected element is temporarily fixed on the same propagation environment from the base station. Cancellation of movement of the receiving point can then be achieved.

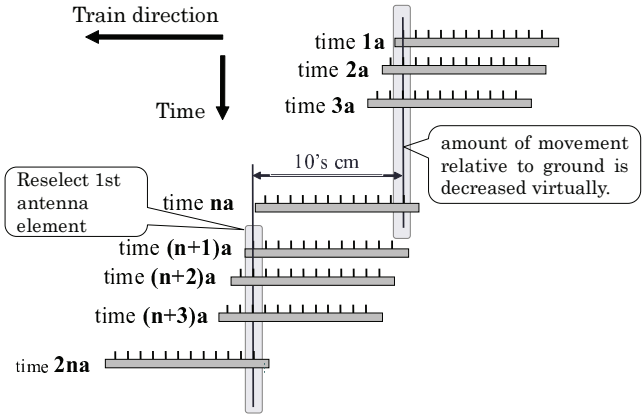

Fig. 2. Switched antenna array concept.

The length of the antenna array determines the duration of the movement-cancellation. The first element is reselected once the selected element reaches the last antenna element, and at that moment in time the propagation environment is considerably altered. This return-to-start switch timing should synchronize with a channel estimation period or boundary between two OFDM symbols or frame in order to prevent a degradation in the data rate caused by an erroneous channel compensation. The switching frequency f_{sw} (Hz) is calculated in Eq. (1).

$$f_{sw} = \frac{v}{d}, \tag{1}$$

where v (m/s) is the velocity of antenna array, and d (m) is the distance between antenna elements.

III. Switched Antenna Array

The electrical circuit schematic for the system is shown in Fig. 3. Two four-to-one radio frequency (RF) switches are controlled by a FPGA based control circuit. In a single channel mode, the circuit enables one of the elements to be routed to the recorder. In a dual channel operation, two adjacent elements are concurrently selected and their signals recorded. This allows interpolation in between two adjacent antenna elements to improve the accuracy. The switch insertion loss is about 2.5 dB and the measured total loss between the antenna port and input port of the receiver is between 3.5 dB to 4.0 dB.

The antenna array movement is controlled by a stepping motor in order to keep an accurate and constant velocity. The antenna array progresses along a 5 m section of linear track at a set speed of 3.6 km/h. Due to the finite time required for the array to accelerate to the desired speed and decelerate to a stop afterwards, the section length of constant speed is approximately 4 m.

The experiment measurements were made in an anechoic chamber to enable repeatability of results by eliminating the unwanted multipath. A view of the mounted antenna array moving along the rail is shown in Fig. 4. The parameters of the experiment are listed in Table I.

TABLE I. Experiments parameters.

Item	Value
Center Frequency	2.5 GHz
Physical speed	3.6 km/h
Transmit signal	QPSK, CW
Tx antenna	Horn (17 dBi)
Rx antenna	8 dipoles (@ 2.5 dBi)
Rx Element spacing	{1/4, 3/8, 1/2, 5/8, 3/4}λ

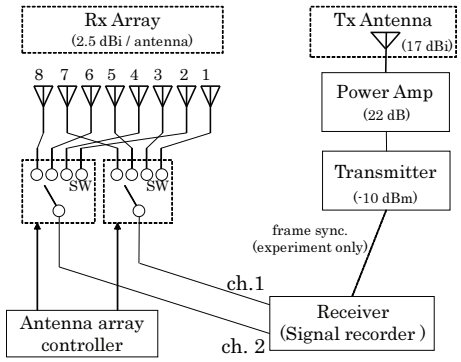

Fig. 3. Schematic of the switching array system.

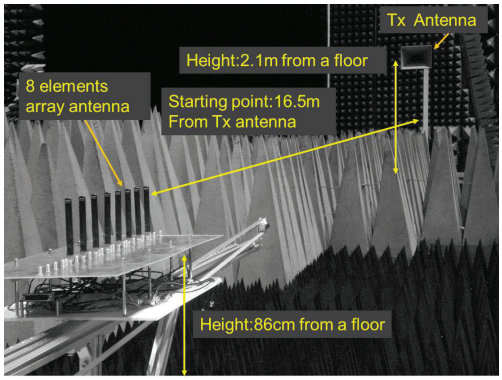

Fig. 4. A setup of the experiment in the anechoic chamber.

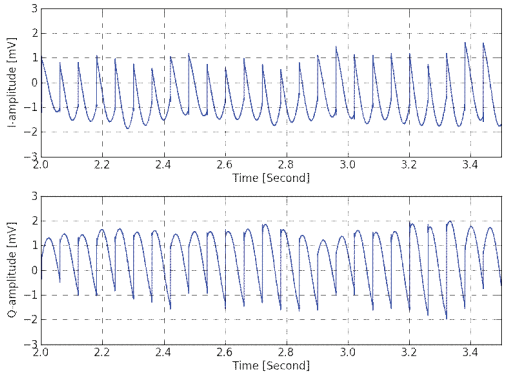

Fig. 5. Output signal of 1/2 λ spacing array antenna moving at 3.6 km/h with 16.67 Hz switching.

A. Doppler characteristics

The offset between the transmitter carrier and receiver local frequency was first corrected using a hardware frequency offset correction function. A continuous wave (CW) signal is transmitted and the received signal is converted into the frequency domain through the FFT operation in order to examine the Doppler characteristics. In the static case, the recovered signal voltage was therefore observed to be constant. In the moving state, a Doppler shift is observed as a sine wave. Once continuous switching of the antenna elements starts, this sine wave is canceled. In this case, eight times repetition of almost the shape is seen in Fig. 5 due to the eight elements.

The spectrum of the received signal in the static case is shown in Fig. 6 (left). A peak at 0 Hz is observed because the transmit signal is a CW. The spectrum during movement without switching is shown next in Fig. 6 (right). Only a single Doppler shift of 8.3 Hz is observed as shown in the figure. Once switching of the elements has started, the peak frequency shifts to -8.3 Hz, and switching-noise with many harmonics are observed as shown in Fig. 7. Some switching noise can additionally be seen but this can be filtered out for a production model as part of our future work.

Once switching of the antenna elements starts, the peak returns to 0 Hz with some switching-noise observed as shown in Fig. 8, and indicates that the proposed movement-cancellation receiver can be achieved. The spacing between elements is an important consideration. If the spacing is too large, the Doppler shift will be compensated at less frequent intervals. On the other hand, too short a spacing leads to mutual coupling and can cause unwanted directivity. The effect of increased spacing is shown in Fig. 9. In the case of 1/4λ, there is a larger difference in received power between the first and other elements and a more asymmetrical spectral response is observed compared with that for 1/2λ in Fig. 8. In the case of 3/4λ, it was observed that the adjacent peak occurs at $\pm$11 Hz which is twice as near compared to $\pm$22 Hz with 1/2λ spacing and hence a sharper filter is required.

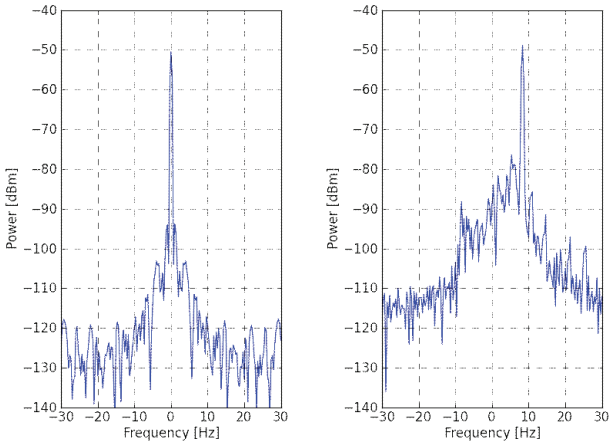

Fig. 6. Spectrum of received signal in static (left) and moving at 3.6 km/h (right) without switching.

IV. WiMAX System

To demonstrate the effectiveness of the proposed system an end-to-end WiMAX performance simulation was made. The WiMAX implementation is based on the fixed IEEE802.16-2004 standard which employs the 256-point FFT in a 5 MHz bandwidth. Special features of WiMAX systems include long communication distance, high-data rates, quality of service provision, and bandwidth scalability (1.25 MHz to 20 MHz) [10] [11]. WiMAX employs the Orthogonal Frequency Division Multiplexing (OFDM) technique that divides the transmission bandwidth into many narrowband sub-channels. These sub-channels experience almost flat fading across their band and are easily equalized with a division operation per sub-carrier.

A. Transmitter

The WiMAX baseband system block diagram is shown in Fig. 10. At the transmitter pseudo-random input data is scrambled to eliminate occurrences of long sequences of the same binary digits. The data is then Reed-Solomon (RS) block encoded, and convolutionally encoded for forward error

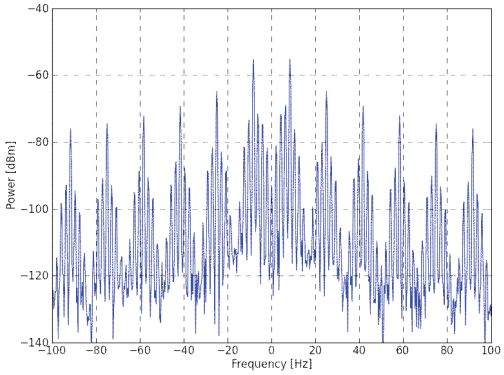

Fig. 7. Spectrum of 1/2 λ spacing array antenna in static state with 16.67 Hz switching.

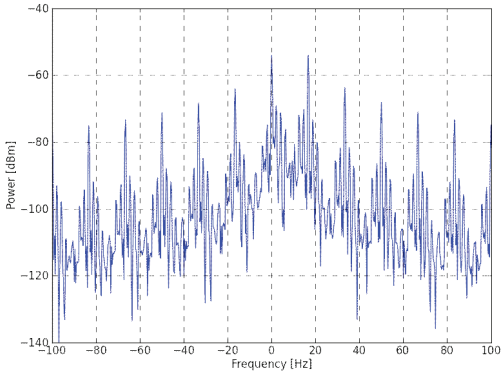

Fig. 8. Spectrum of 1/2 λ spacing array antenna moving at 3.6 km/h with 16.67 Hz switching.

correction. The interleaver distributes bits across the entire bandwidth as a fading counter-measure. The frequency domain data is then modulated, and converted into the time-domain using the IFFT operation and a cyclic prefix of length longer than the maximum multipath delay added. The frame structure is shown in Fig. 12. The first two OFDM symbols comprise a known preamble for timing recovery purposes. We have inserted an additional OFDM symbol consisting of complex +1,-1 frequency domain symbols and used this to estimate the channel at the start of the frame. The next N-3 symbols are data symbols with a final end of frame symbol inserted.

The data frames are computed off-line and written to file as shown in Fig. 11. An Agilent Vector Signal Generator is connected to a PC running Agilent Signal Studio software and up-converts the baseband data to RF. The transmission symbol rate was set at 5.6 MSa/s. When the first antenna of the train reaches a predetermined start position, data transmission starts and the receiver starts sampling.

B. Receiver

The sample rate at the receiver is set at 11.2 MSa/s. The signals are received by the switched-antenna array, sampled using an in-house developed NI/Labview system. The baseband data is stored in binary format and decoded using the

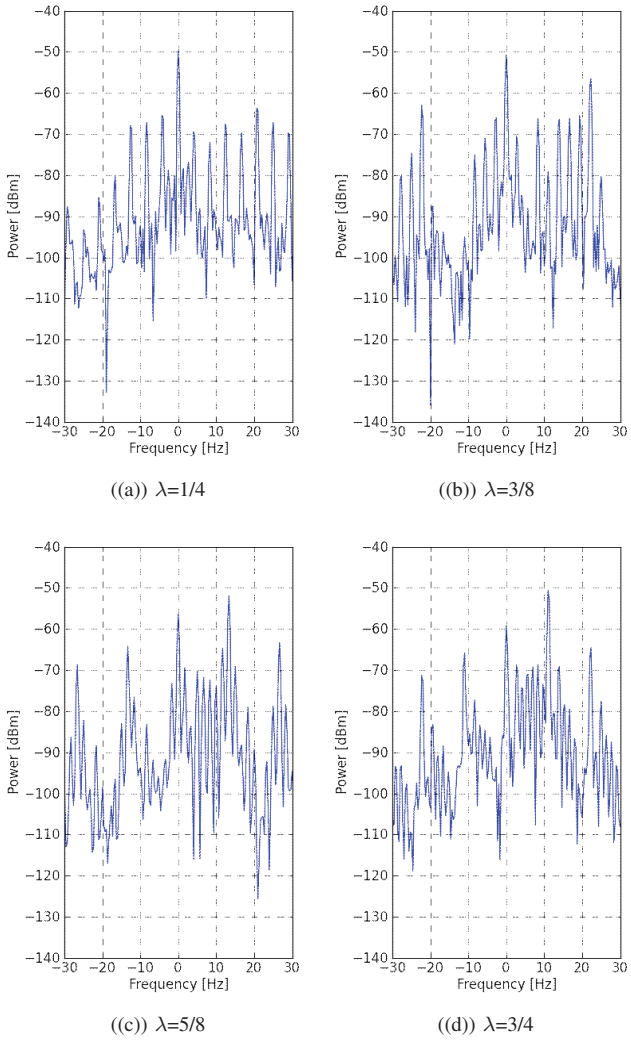

Fig. 9. Spectrum for different element spacing moving at 3.6 km/h with switching $f_s w$.

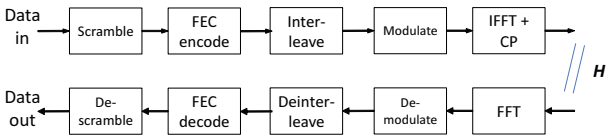

Fig. 10. WiMAX transmitter and receiver block diagrams.

WiMAX simulator. The start of frame is found through cross-correlation with the known preamble. The inverse operations of the transmitter are then computed. The time domain data is converted into the frequency domain using the FFT. The symbols are demodulated into bits, deinterleaved, FEC decoded and finally descrambled.

The antenna element switching rate for the results presented here was 16.67 Hz. The base Tx symbol rate was 5.6 MHz and represents the actual physical speed of 3.6 km/h. By reducing the transmission symbol rate to 560 kHz and there-

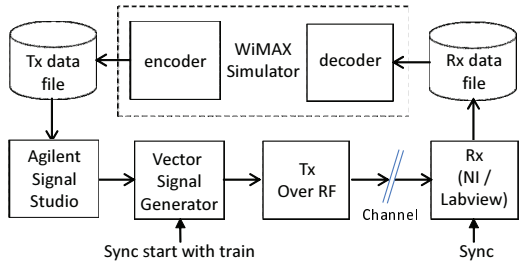

Fig. 11. WiMAX Tx and Rx simulation process.

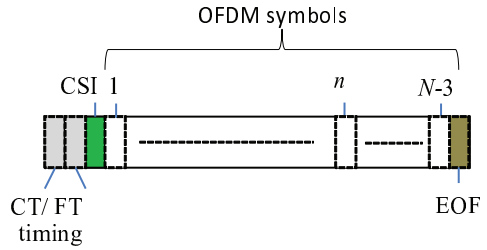

Fig. 12. Frame structure.

fore increasing the amount of fading within a symbol, an equivalent fading speed of 36 km/h was produced. At the speed of 3.6 km/h there are approximately seventy frames per antenna switching period, whilst at the virtual speed of 180 km/h the transmission rate is reduced by a factor of 50 and there are approximately 1.4 frames per switching period as shown in Table II.

C. Non-switching

Here, a conventional channel estimation is made at the start of each frame on channel 1 and an interpolation made at each OFDM symbol to track the phase rotation due to movement. The interpolated CSI at OFDM symbol n on sub-carrier k is estimated according to Eq. (2).

$$H_n^k = \left(\frac{N-n}{N}\right) H_L^k + \left(\frac{n}{N}\right) H_{L+1}^k, \tag{2}$$

where H_L^k and H_{L+1}^k are the CSI estimates obtained using the preamble in two successive frames, and N is the number of symbols per frame.

D. Switching

The switching of the antennas is recorded on two adjacent channels simultaneously enabling the signal to be known at both the start and end of each antenna switching period. With switching, the Doppler shift is canceled at the antenna switching instance. In between these two points there is some residual movement which is reduced by interpolation. The element switching sequence and relative frame duration for the physical 3.6 km/h ($\times 1$) and 180 km/h ($\times 50$) virtual speeds are shown in (Fig. 13). The figure also shows that by doubling the element sampling time on each channel, the switching noise can be reduced.

The two signals s_1 and s_2 from each channel are combined as

$$s = w_1\ s_1 + w_2\ s_2, \tag{3}$$

where w_1 and w_2 are linear weights whose values are proportional to the distance traversed between the two elements. The received real component on Chan. 1, s_1 and the interpolated real component of s are plotted in Fig. 14.

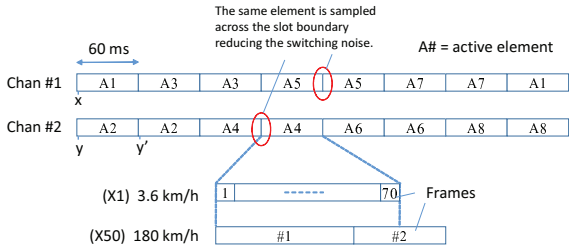

Fig. 13. Relative antenna switching and frame duration at 3.6 km/h and 180 km/h. The switching noise is reduced by doubling the element sampling time on each channel.

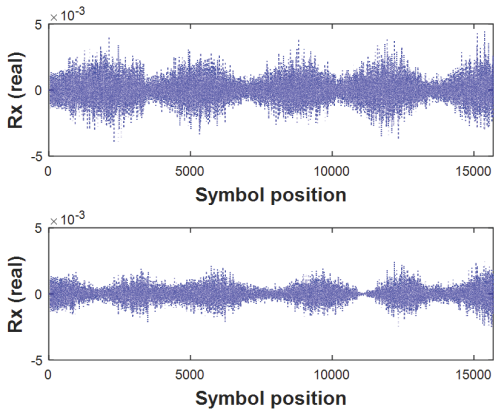

Fig. 14. (Top) Received real signal on the Chan #1 and (Bottom) interpolated real signal.

TABLE II. Antenna and frame timing.

Item	Value		
Symbol rate (TX)	5.6 MHz	560 kHz	112 kHz
Physical Speed		3.6 km/h	
Virtual Speed	3.6 km/h	36 km/h	180 km/h
Element switch rate		16.67 Hz	
Element switch duration		60 ms	
Frame duration	0.86 ms	8.6 ms	42.9 ms
Frames per element switch	70	7	1.4
OFDM symbols per frame		11	

E. Experimental results

Experimental data was collected for two principle situations: a) conventional set-up using single non-switched moving receiver and b) moving receiver with antenna switching applied. The virtual speeds were 36 km/h and 180 km/h. In our initial experiments the frame start positions are independent

of the train speed and therefore some CSI or data symbols coincide with the return-to-start switching transition. These symbols were excluded from the BER calculation as in a final implementation such transitions would be timed to not occur. The BER performance showing the improvement of the proposed scheme is plotted in Fig. 15. The current results do not include the effect of multipath fading, and as each path can have a different Doppler shift, it is expected that further performance gains will be made in such environments.

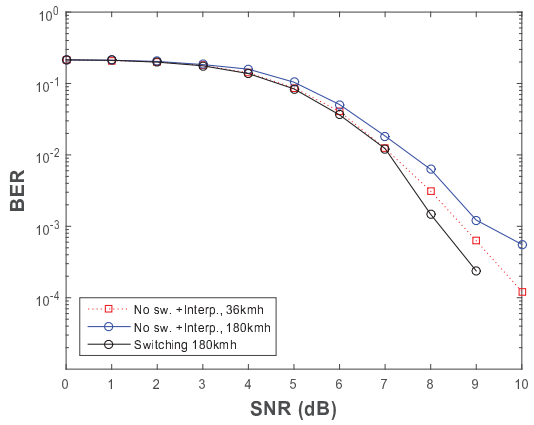

Fig. 15. BER performance with i) no switching with interpolation and ii) switching.

V. Further Work

Performance measurements at the extended speed of 360 km/h are currently under investigation. The effect of element spacing with respect to mutual coupling and switching noise in an outdoor environment can be studied. The antenna array direction relative to the transmitter beam pattern should also be investigated. We are planning to investigate the performance with lower-profile patch antennas and also evaluate the benefits of deploying a larger number of antenna elements.

VI. Conclusions

An experimental scale-model system employing a switched antenna concept was developed in order to reduce the effect of fast-fading experienced by vehicles traveling at high speeds. The Doppler frequency shift on a CW signal was successfully canceled by switching the elements in the reverse direction of motion. The results show that the performance of an OFDM system in a fading environment can be improved through the antenna switching. Further work will investigate the performance at higher speeds, in a multipath environment and with different numbers and types of antenna elements.

Acknowledgment

This work was supported by the Ministry of Internal Affairs and Communications SCOPE (Strategic Information and Communications R&D Promotion Programme) 2015 (Grant number 135007103).

References

[1] "ARIB 2020 and Beyond Ad Hoc Group White Paper Mobile Communications Systems for 2020 and beyond," *Association of Radio Industries and Businesses (ARIB)*, Oct. 2014.

[2] S. Knorzer, M. Baldauf, T. Fugen and W. Wiesbeck "Channel analysis for an OFDM-MISO train communications system using different antennas," *Proc. IEEE VTC*, 2007.

[3] E. Masson, M. Chennaoui, M. Berbineau, and H. Dumortier, "Performance of High Data Rate Transmission Scheme developed for train communications," *IEEE 7th International Conference on Intelligent Transport Systems Telecommunications, (ITST 2007)*, 2007.

[4] J. Kim, S. Choi and I. Kim "A shared RUs based distributed antenna system for High-Speed Trains," *Proc. IEEE ISCE*, 2014.

[5] B. Ouarzazi, M. Berbineau, I. Dayoub and A. Menhaj-Rivenq, "Channel estimation of OFDM system for high data rate communications on mobile environments," *IEEE 9th International Conference on Intelligent Transport Systems Telecommunications, (ITST 2009)*, pp 425–429, 2009.

[6] Z. Min, W. Muqing, S. Yanzhi, J. Guiyuan et al., "Analysis and Modeling of the LTE Broadband Channel for Train-Ground Communications on High-Speed Railway," *IEEE Vehicular Technology Conference (VTC Fall 2013)*, 2013.

[7] M. Tseng and M. Cheng, "Experimental Study of Fading Characteristics for Wireless Communications in High-Speed Railway Environments," *IEEE Antennas and Propagation Society International Symposium (APSURSI)*, 2012.

[8] E. Yaacoub, "Enhanced Connectivity in Railroad Networks using LTE Relays with Directive Antennas," *IEEE IEEE GCC Conference and exhibition*, Doha, Qatar, Nov. 17-20, 2013.

[9] S. Tsukamoto, Y. Hou, M. Ariyoshi, R. Baba, S. Yamamoto, S. Aikawa "Sequentially Switched Antenna Array Receiver - Enhancing Data Transmission Rate on High Speed Vehicles," *B-1-220*, March 2014.

[10] "IEEE 802.16: WiMAX Overview, WiMAX Architecture," *International Journal of Computer Theory and Engineering*, vol. 5, no. 5, Oct. 2013.

[11] K. Etemad, "Overview of Mobile WiMAX Technology and Evolution," *IEEE Communications Magazine*, pp. 31–40, Oct. 2008.